CHEMISTRY
A EUROPEAN JOURNAL

DOI: 10.1002/chem.200801106

VIP

Self-Assembly of Alkyl-Substituted Cubic Siloxane Cages into Ordered Hybrid Materials

Atsushi Shimojima,*[a] Ryota Goto,[b] Norimasa Atsumi,[b] and Kazuyuki Kuroda*[b, c]

Abstract: Siloxane-organic hybrids with well-ordered mesostructures were synthesized through the self-assembly of novel amphiphilic molecules that consist of cubic siloxane heads and hydrophobic alkyl tails. The monoalkyl precursors functionalized with ethoxy groups ($C_nH_{2n+1}Si_8O_{12}(OEt)_7$, **1C*n***, $n=$ 16, 18, and 20) were hydrolyzed under acidic conditions with the retention of the siloxane cages, leading to the formation of two-dimensional hexagonal phases by evaporation-induced self-assembly processes. Analysis of the solid-state ^{29}Si MAS NMR spectra of these hybrid mesostructures confirmed that the cubic siloxane units were cross-linked to form siloxane networks. Calcination of these hybrids gave mesoporous silica, the pore diameter of which varied depending on the alkyl-chain length. We also found that the precursors that had two alkyl chains formed lamellar phases, thus confirming that the number of alkyl chains per cage had a strong influence on the mesostructures. These results expand the design possibility of novel nanohybrid and nanoporous materials through the self-assembly of well-defined oligosiloxane-based precursors.

Keywords: amphiphiles · mesoporous materials · nanostructures · self-assembly · silica-based hybrid

Introduction

The self-assembly of molecular building blocks into well-defined architectures has received considerable interest as a promising approach to nanomaterials synthesis.[1] Recently, various organosilane-based molecules have been found to form nanostructured silica-based hybrids owing to the amphiphilic nature of hydrolyzed species[2–4] or to the specific interactions, such as hydrogen bonding and π–π interactions between organic groups.[5–7] In addition to monomeric precursors with the general formula of $R'Si(OR)_3$ or $(RO)_3Si$-R'-$Si(OR)_3$, the use of oligosiloxane precursors consisting of both $CSiO_3$ and SiO_4 units will lead to diverse compositions and structures.

We have reported the formation of hybrid mesostructures, 2D hexagonal ($n=6$–10), 2D monoclinic ($n=12$ and 13), and lamellar ($n=14$–18), from oligosiloxane precursors consisting of an alkyl chain and a branched tetrasiloxane unit ($C_nH_{2n+1}Si(OSi(OMe)_3)_3$, hereafter called "tetrasiloxane precursors").[8] Such an approach based on the use of single hybrid precursors promises to produce mesostructured hybrid materials with uniform distribution and configuration of organic groups without phase-separation. Furthermore, we can expect the construction of mesostructures with molecularly designed siloxane networks, which is very important for a wide range of applications such as catalysis. However, the aforementioned tetrasiloxane precursors underwent intramolecular rearrangement during hydrolysis of alkoxy groups,[8b] which hampered the precise design of the siloxane networks at the molecular scale.

The cubic octasiloxane cage, Si_8O_{12}, appears to be suitable as an oligosiloxane unit because of its distinctive features, such as rigidity, high symmetry, and functionalization capability. Previously, siloxane cage compounds ($R_8Si_8O_{12}$, R = H, O^-, OCH_3, and organic groups) have been widely used as

[a] Prof. A. Shimojima
Department of Chemical System Engineering
The University of Tokyo, Hongo-3
Bunkyo-ku, Tokyo 113–8656 (Japan)
Fax: (+81) 3-5800-3806
E-mail: shimoji@chemsys.t.u-tokyo.ac.jp

[b] R. Goto, N. Atsumi, Prof. K. Kuroda
Department of Applied Chemistry
Waseda University, Ohkubo-3
Shinjuku-ku, Tokyo 169–8555 (Japan)
Fax: (+81) 3-5286-3199
E-mail: kuroda@waseda.jp

[c] Prof. K. Kuroda
Kagami Memorial Laboratory for Materials Science and Technology
Waseda University, Nishiwaseda-2
Shinjuku-ku, Tokyo 169–0051 (Japan)

Supporting information for this article is available on the WWW under http://dx.doi.org/10.1002/chem.200801106.

WILEY InterScience DISCOVER SOMETHING GREAT
© 2008 Wiley-VCH Verlag GmbH & Co. KGaA, Weinheim

nanobuilding blocks of silica-based materials.[9] Ordered nanocomposites have been constructed by the surfactant-directed self-assembly process[10–12] and by the layer-by-layer assembly process.[13] Several attempts have also been made in the design of organically-modified octasiloxane cage capable of self-assembly, e.g., i) thermotropic liquid crystalline molecules having Si_8O_{12} cores,[14] ii) polyimide-based copolymers grafted or end-capped with $R_7Si_8O_{12}$ (R = cyclohexyl),[15] and iii) amphiphilic molecules in which hydrophilic chains such as oligo(ethyleneoxide) is bonded to $R_7Si_8O_{12}$ (R = H or Et) units.[16] However, most of these studies utilized silsesquioxane cages $(CSiO_{1.5})_8$, lacking the ability to form siloxane networks due to the absence of alkoxysilyl (SiOR) groups, and the design of the cubic siloxane-based molecules that produce well-ordered mesostructures consisting of cross-linked siloxane cages has been unprecedented.

Herein, we report the design of novel alkyl-substituted cubic siloxane cages functionalized with alkoxy groups that become amphiphilic upon hydrolysis. Although various mono-substituted cages, including $C_6H_{13}(H_7)Si_8O_{12}$,[17,18] have previously been reported, self-assembly of alkyl-substituted cubic siloxane cages has only been studied by computer simulation.[19] In the present work, self-assembly and subsequent polycondensation of amphiphilic molecules that have a hydrophilic cage structure are experimentally verified for the first time. We found that the monoalkyl-substituted precursors (**1C*n***) in Scheme 1) formed 2D hexagonal mesostructures with cylindrical assemblies, consisting of networks of the cages. We also examined the use of dialkyl-substituted precursors. The formation processes and the structures of these hybrid mesostructures are described.

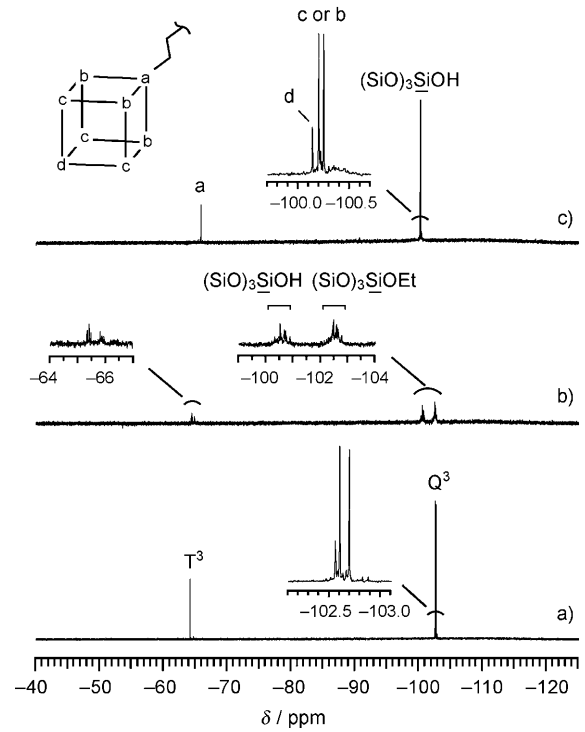

Figure 1. Liquid-state ^{29}Si NMR spectra of a) **1C16** and the solutions after b) 1 day and c) 7 days of reaction.

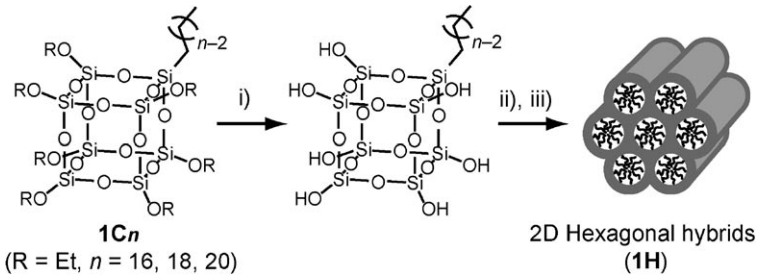

Scheme 1. Formation of hybrid mesostructure (**1H**) from monoalkyl-substituted cubic siloxanes (**1C*n***) by i) hydrolysis, ii) evaporation-induced self-assembly, and iii) polycondensation.

Results and Discussion

Hydrolysis of **1C*n*** without cross-linking is crucial for subsequent self-assembly induced by evaporation of the solvent. We first studied the hydrolysis processes of **1C*n*** by liquid-state ^{29}Si NMR. Figure 1 shows the ^{29}Si NMR spectra of **1C16** and the solutions after 1 and 7 days of reaction. The unreacted **1C16** exhibits four signals corresponding to the T^3 ($CSi(OSi)_3$) site and three inequivalent Q^3 ($Si(OSi)_3(OEt)$) sites (Figure 1a). After 1 day of reaction (Figure 1b), several unresolved signals are observed at around $\delta = -65.5$, -100.5 and -102.5 ppm. The signals at around $\delta = -100.5$ ppm arise from hydrolysis of SiOEt groups to form SiOH groups.[20] The complexity of this spectrum is attributed to the slight variation in the environments of SiOH, SiOEt and $SiC_{16}H_{33}$ sites depending on the number and position of the SiOH groups. After 7 days (Figure 1c), the signals due to $Si(OSi)_3(OEt)$ almost disappear and the spectrum mainly shows a T^3 signal at $\delta = -65.8$ ppm and three Q^3 signals at $\delta = -100.13$, -100.19 and -100.24 ppm. These signals have an approximate intensity ratio of 1:1:3:3 and are assigned to completely hydrolyzed species (inset of Figure 1c). Similar hydrolysis behaviors were also observed for **1C18** (Supporting Information, Figure S1).

It is interesting to note that the hydrolysis of **1C*n*** proceeds much slower than tetraethoxysilane (TEOS). Under the identical conditions, TEOS was completely hydrolyzed within 0.5 h. Such a large difference can be explained in terms of hydrolysis mechanism: hydrolysis of **1C*n*** should proceed without the inversion of SiO_4 tetrahedra, being in contrast to the S_N2 type reaction proposed for tetraalkoxysilanes.[20] Notably, the hydrolysis of the Si-O-Si linkages is very slow and is confirmed by the appearance of no T^2 or Q^2 signals during the reaction. Furthermore, the absence of the Q^4 signal even after complete hydrolysis of **1C*n*** indicat-

 © 2008 Wiley-VCH Verlag GmbH & Co. KGaA, Weinheim

ed that condensation between the cages was suppressed, which is probably due to steric repulsion between long alkyl chains. Although the small, broad signal centered at $\delta = -100.4$ ppm is indicative of the co-existence of a minor amount of other species, hydrolysis of **1C*n*** proceeded with the retention of the original cage structure. This is one of the specific features of the present self-assembly process, being in clear contrast to the case of branching siloxane units which undergo intramolecular condensation and cleavage of Si-O-Si bonds.[8b]

The hydrolyzed **1C*n*** are amphiphilic molecules, and their self-assembly indeed occurred upon evaporation of the solvent. The xerogel films prepared by drying the fully hydrolyzed solution of **1C*n*** (after 7 days) dropped on glass substrates appear birefringent when viewed under a polarizing microscope. The observed fan-like texture (Figure 2) is typical of a hexagonal columnar mesophase (*p6mm*).[21] A similar hexagonal phase was also obtained from the hydrolyzed solution after 5 days of reaction at which time the degree of SiOEt hydrolysis was ≈70%, as roughly estimated by ^{13}C and ^{29}Si NMR (data not shown), whereas the solution after 3 days of reaction gave an isotropic xerogel. Thus the number of OH groups per cage dominates the amphiphilic self-assembly of hydrolyzed **1C*n***.

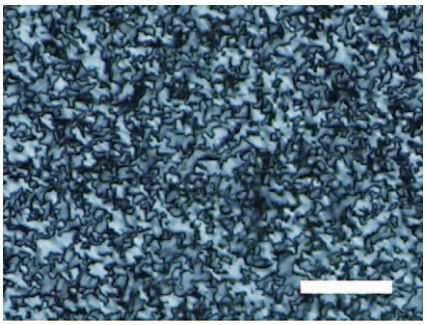

Figure 2. Polarizing microscopy image of the thick film prepared by drying of the hydrolyzed solution of **1C18**. Scale bar: 50 μm.

The 2D hexagonal structure of the products derived from fully hydrolyzed **1C*n*** was actually confirmed by X-ray diffraction (XRD) and transmission electron microscopy (TEM). Figure 3 shows the powder XRD patterns of the pulverized samples (**1H**) before and after calcination. The as-synthesized **1H** ($n = 16$, 18, and 20) exhibit the strongest peaks corresponding to the d_{10} spacings of 3.72, 3.96, and 4.20 nm, respectively (Figure 3, left). Both hexagonal patterns and striped patterns, typical of a 2D hexagonal structure, are observed by TEM (Figure 4, and Figure S2 in the Supporting Information). Note that (11) peaks are not clearly observed in the XRD patterns. This should be a result of the preferential orientation of the plate-like particles originating from the xerogel films in which cylindrical assemblies are aligned parallel to the surfaces.[22] These mesostructures were retained even after calcination (Figure 3, right), although the d_{10} spacing decreased by ≈0.5 nm, owing to the thermal shrinkage of the siloxane networks.

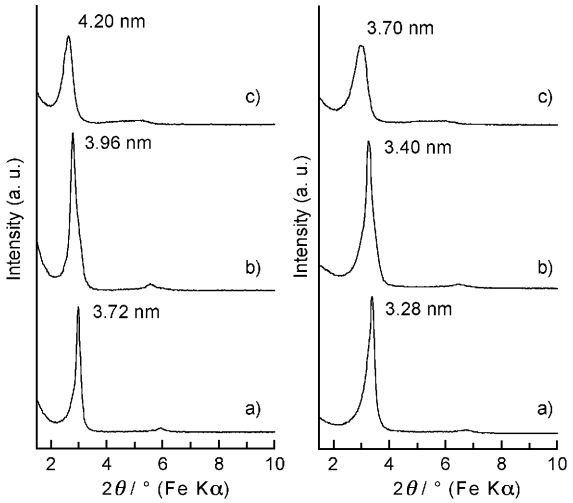

Figure 3. Powder XRD patterns of the hybrids **1H** before (left) and after (right) calcination: a) $n = 16$, b) $n = 18$, and c) $n = 20$.

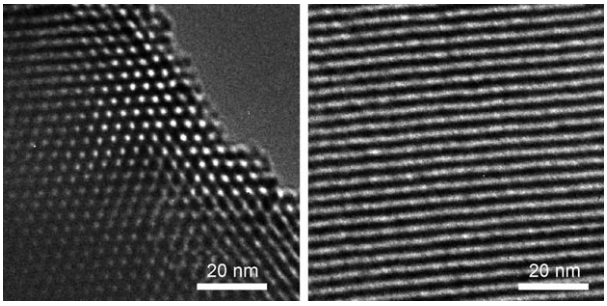

Figure 4. Typical TEM images of the hybrid derived from **1C18** (before calcination) showing the honeycomb (left) and striped (right) patterns.

As we reported previously,[8b] tetrasiloxane precursors ($C_nH_{2n+1}Si(OSi(OMe)_3)_3$) favored the formation of lamellar structures when $n = 14$. The formation of 2D hexagonal structures from **1C*n*** with $n = 16$, 18, and even $n = 20$ can be attributed to the increase of the head group area that generally leads to the formation of higher curvature mesophases.[23] Other mesophases such as 3D cubic and 3D hexagonal phases, both of which comprised of spherical assemblies, might be formed from **1C*n*** with shorter chain length. However, our preliminary experiments suggested that well-ordered structures were not obtained under the present experimental conditions. For example, the hybrid derived from **1C*n*** with $n = 14$ exhibited a single XRD peak ($d = 3.51$ nm) owing to a less-ordered 2D hexagonal structure. The mesostructure became more disordered when $n = 10$ (data not shown).

To further investigate the molecular factor affecting the self-assembly processes, we examined the use of dialkyl precursors ($(C_nH_{2n+1})_2Si_8O_{12}(OEt)_6$, **2C*n***, $n = 16$, 18, and 20), which were obtained as a major by-product (≈25% yield). As shown in Figure 5, there are three possible isomers of di-

 © 2008 Wiley-VCH Verlag GmbH & Co. KGaA, Weinheim

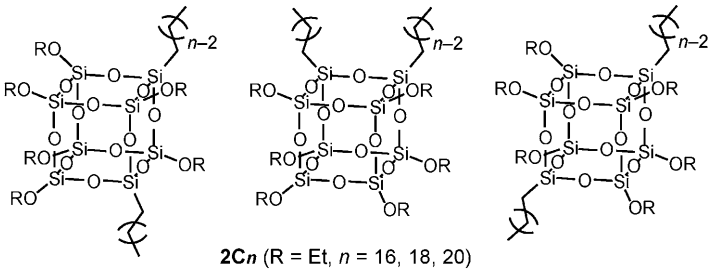

Figure 5. Three possible isomers of dialkyl-substituted cubic siloxane cages (**2Cn**).

alkyl-substituted cages. The GPC chromatographs of **2Cn** showed single peaks with shorter retention times than **1Cn** (data not shown). The presence of three isomers in each precursor was indeed suggested by NMR: i) the ^{29}Si NMR spectrum consists of three T^3 signals and six Q^3 signals, ii) the ^{13}C NMR spectrum shows three $SiCH_2$ signals, and iii) the ^{1}H NMR spectrum shows the CH_2OSi/CH_2Si ratio of 3 (see the Supporting Information).

Although the separation of these isomers was unsuccessful, single mesophases were obtained from the mixtures. Hydrolysis and polycondensation of **2Cn** led to the formation of lamellar hybrids (**2H**) independent of the alkyl chain length. The XRD patterns show the peaks with $d=3.46$, 3.60, and 3.88 nm when $n=16$, 18, and 20, respectively (Figure 6), and these peaks disappeared after calcination, owing to the collapse of the structure. The lamellar structure of **2H** was also supported by their swelling behavior; the d spacings were increased ($\Delta d=0.5$ nm for $n=18$) when the samples were treated with decyl alcohol.

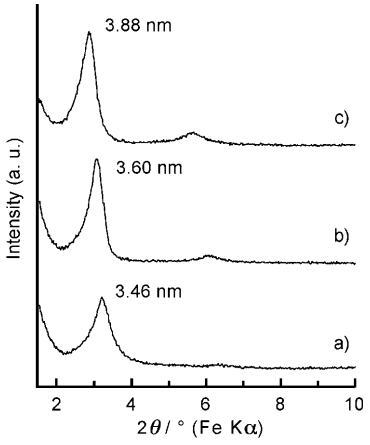

Figure 6. Powder XRD patterns of the lamellar hybrids (**2H**) derived from **2Cn**: a) $n=16$, b) $n=18$, and c) $n=20$. These samples were prepared with a molar ratio of **2Cn**/THF/H_2O/HCl = 1:75:18:0.5. Other experimental conditions were identical to those for the preparation of **1H**.

Solid-state ^{29}Si NMR analysis gave us information about the siloxane networks in the hybrid solids. The ^{29}Si MAS NMR spectra of **1H** and **2H** ($n=18$), are shown in Figure 7a,b, respectively. Both spectra consist of five signals at

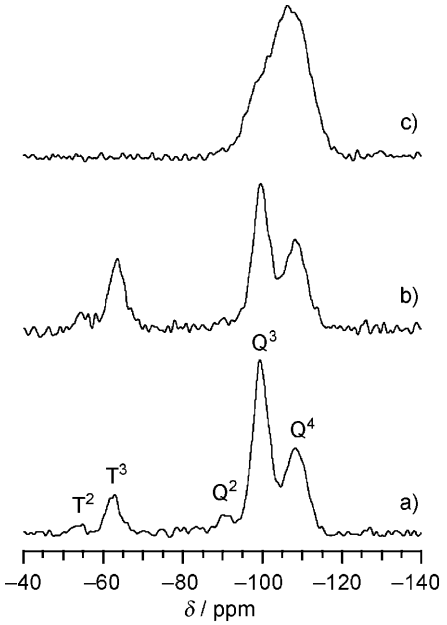

Figure 7. Solid-state ^{29}Si MAS NMR spectra of a) **1H** ($n=18$) before calcination, b) **2H** ($n=18$) before calcination, and c) **1H** ($n=18$) after calcination.

$\delta=-55$, -64, -91, -100, and -109 ppm, corresponding to the T^2, T^3 (T^x, $CSi(OSi)_x(OH)_{3-x}$), Q^2, Q^3 and Q^4 units (Q^y, $Si(OSi)_y(OH)_{4-y}$), respectively. The T/Q ratios are consistent with those in **1C18** (T/Q = 1/7) and **2C18** (T/Q = 1/3). The appearance of the Q^4 signal indicates the formation of the siloxane networks of the octasiloxane cages. In the case of **1H**, on the basis of the relative intensity ratio of the Q^4 signal ($Q^4/(Q^2+Q^3+Q^4)=0.39$), the average number of cage corners linked to other cages is calculated to be 2.7 per cage.

The presence of small T^2 and Q^2 signals in Figure 7a,b is indicative of partial cleavage ($\approx 8\%$) of siloxane bonds during polycondensation. Such cleavage was also reported for the sol–gel processes of a methoxy-derivative of cubic siloxane cage ($Si_8O_{12}(OMe)_8$).[24] However, the high T^3/T^2 ratios of **1H** and **2H** suggests that the cage units are at least partly retained in the hybrid mesostructures. In fact, the hybrids derived from the mixtures of long-chain alkyltrialkoxysilane and tetraalkoxysilane predominantly contain the T^2 units because of the steric repulsion between long alkyl chains.[2b] The situation is the same even when tetrasiloxane precursors having T^3 units was used as the precursor, because partial cleavage of the Si-O-Si bonds occurred during the reaction.[8] Further support was obtained by FT-IR analysis of **1H** (Supporting Information, Figure S3). The spectrum clearly shows the band at $\tilde{\nu}\approx 580$ cm^{-1} which is typically observed for the siloxane-based materials containing double-four-membered rings.[11,12,25] It appears, however, that the cages are randomly arranged because XRD peaks assignable to short-range order were not observed.

Such a bottom up approach to control the structure of siloxane networks is potentially very important for the practi-

 © 2008 Wiley-VCH Verlag GmbH & Co. KGaA, Weinheim

cal applications concerning the porosity, density, and refractive index of silica. Klemperer et al. reported the formation of high-surface-area silica xerogels from $Si_8O_{12}(OMe)_8$.[24] It was proposed that the rigidity of the cubic-siloxane unit inhibited extensive cross-linking, thereby generating porosities. However, in the case of the as-synthesized **1H**, there was no porosity measurable by N_2 adsorption (data not shown), which is suggestive of denser siloxane networks in **1H**. This result may arise from the differences in the reaction conditions and/or in the composition of the reaction mixtures.

The ^{29}Si MAS NMR spectrum of **1H** after calcination (Figure 7c) shows broad signals corresponding to the Q^3 and Q^4 units, suggesting that the $CSiO_3$ (T) unit was converted to SiO_4 (Q) unit by thermal cleavage of Si–C bonds. The relative intensity ratio of the Q^4 signal ($Q^4/(Q^2+Q^3+Q^4)$) increased from 0.39 to 0.78, indicating that further condensation between residual silanol groups occurred. The complete removal of organic moieties was confirmed by IR (Figure S3 in the Supporting Information). Also noted is that the significant change in the profile of the IR spectrum at around $\tilde{\nu}=550\ cm^{-1}$, which is possibly a result of shrinkage of the siloxane networks and/or structural deformation of cubic siloxane units by calcination.

As expected from the fact that the calcined **1H** retained the 2D hexagonal structures, they were found to have ordered mesopores. Figure 8 shows the nitrogen adsorption-

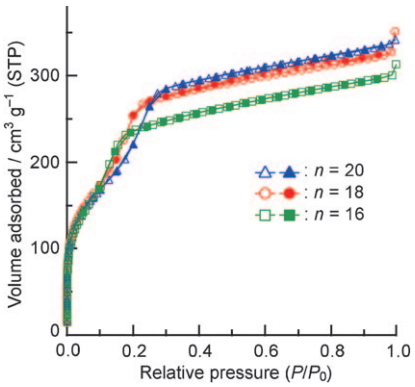

Figure 8. Nitrogen adsorption-desorption isotherms of **1H** after calcination. Open symbols and filled symbols denote adsorption and desorption branches, respectively.

desorption isotherms for **1H** after calcination. These samples show type IV isotherms characteristic of mesoporous silica. The BET surface area, pore volume, and average pore diameter evaluated by the non-local density functional theory (NLDFT) method are listed in Table 1. The surface areas and the pore volumes are relatively lower than those for the mesoporous silica derived from the tetrasiloxane precursors (e.g., 830 $m^2 g^{-1}$ and 0.58 $cm^3 g^{-1}$, respectively, when the pore size was 3.2 nm).[8b] This should be explained by thicker siloxane walls, owed to the increased number of Si atoms per alkyl chain. Actually, the wall thicknesses calculated from the pore diameters and the interpore distances (calculated from the d_{10} spacings) for the calcined **1H** are 0.93–0.98 nm, being larger than that for the above mentioned mesoporous silica (0.67 nm).[8b] Such an increase in the pore wall thickness may contribute to the enhanced hydrothermal stability, which is of practical importance.

Table 1. Pore parameters of **1H** after calcination calculated from the N_2 adsorption-desorption isotherms.

Sample	BET surface area [$m^2 g^{-1}$]	Pore volume [$cm^3 g^{-1}$]	Pore diameter [nm][a]
1H ($n=16$)	650	0.41	2.8
1H ($n=18$)	670	0.46	3.0
1H ($n=20$)	660	0.47	3.3

[a] evaluated by using NLDFT.[26]

Conclusion

We have demonstrated the self-assembly of amphiphilic, alkyl-substituted octasiloxane cages into ordered siloxane-based hybrid materials. To the best of our knowledge, this is the first report on the use of a cubic octasiloxane cage as the hydrophilic head of amphiphilic molecules. Two different mesostructures have been formed depending on the number of alkyl chains per cage. Monoalkyl-substituted cages led to the formation of 2D hexagonal mesostructures, which were converted into mesoporous silica by calcination, whereas dialkyl-substituted cages favored the formation of lamellar phases. The liquid-state and solid-state ^{29}Si NMR and IR results suggested that the cage structure was at least partly retained in the hybrid materials. The elaboration of other types of cubic siloxane cages, such as those having double-three and double-five membered rings, will allow the creation of hybrid mesostructures with unique structures and properties. Integration of other metallic species in the cage framework is also important for catalytic applications.

Experimental Section

Synthesis of monoalkyl-substituted precursors ($C_nH_{2n+1}Si_8O_{12}(OEt)_7$, $n=16$, 18, and 20, 1Cn): The precursors **1C*n*** were synthesized by Pt-catalyzed hydrosilylation of 1-alkenes ($CH_2=CH(CH_2)_{n-3}CH_3$, $n=16$, 18, and 20) with $H_8Si_8O_{12}$, followed by the reaction of residual seven Si–H groups with ethanol. $H_8Si_8O_{12}$ was synthesized from $HSiCl_3$ (Tokyo Kasei Kogyo) by using the method reported by Agaskar.[27] Hydrosilylation was performed by the addition of an acetonitrile solution of $H_2PtCl_6{\cdot}6H_2O$ (0.02 M, Kanto Kagaku) to a mixture of $H_8Si_8O_{12}$, 1-alkene (Tokyo Kasei), and toluene (50 mL per 1 g of $H_8Si_8O_{12}$). The molar ratio of $H_8Si_8O_{12}$/1-alkene/$H_2PtCl_6{\cdot}6H_2O$ was $1:1:8\times10^{-4}$. After the mixture was stirred at 100 °C for 1 day under N_2 atmosphere, the solvents were removed in vacuo. The resulting waxy solids consisted mainly of mono- and di-addition products, along with unreacted $H_8Si_8O_{12}$. The mono-addition products, $C_nH_{2n+1}(H_7)Si_8O_{12}$, were isolated by gel permeation chromatography (GPC) using chloroform as the eluent (waxy solids, yield: ≈40% based on $H_8Si_8O_{12}$). Derivatization of $C_nH_{2n+1}(H_7)Si_8O_{12}$ with ethanol (dried) was performed in the presence of $(C_2H_5)_2NOH$ (Tokyo Kasei)[28] with the molar ratio of $C_nH_{2n+1}(H_7)Si_8O_{12}$:EtOH:$(C_2H_5)_2NOH=1:21:0.01$. The

 © 2008 Wiley-VCH Verlag GmbH & Co. KGaA, Weinheim

mixture of $(C_2H_5)_2NOH$ and ethanol was added to the toluene solution (50 mL g^{-1}) of $C_nH_{2n+1}(H_7)Si_8O_{12}$, and the mixture was stirred at room temperature for 16 h under N_2 flow. In this step, special care was taken to minimize water contamination that causes hydrolysis of Si-H. The removal of solvent and residual ethanol in vacuo afforded clear and viscous liquids. Finally, **1C*n*** was purified by GPC (yields: ≈70% based on $C_nH_{2n+1}(H_7)Si_8O_{12}$). Selected data for **1C18**: $C_{18}H_{37}Si_8O_{12}(OEt)_7$: clear, colorless oil. ^{1}H NMR (500 MHz, $CDCl_3$): δ = 0.70–0.74 (t, 2H), 0.87–0.89 (t, 3H; $CH_2CH_2CH_3$), 1.24–1.27 (m, 51H), 1.42–1.45 (m, 2H), 3.87–3.92 ppm (m, 14H; OCH_2); ^{13}C NMR (125.7 MHz, $CDCl_3$): δ = 11.23, 14.13, 17.79, 17.81, 22.42, 22.73, 29.27, 29.40, 29.54, 29.70, 29.73, 31.97, 32.65, 59.86, 59.92, 59.95 ppm; ^{29}Si NMR (99.3 MHz, $CDCl_3$): δ = −64.17 (T^3), −102.58 (Q^3), −102.63 (Q^3), −102.72 ppm (Q^3); MS (FAB): *m*/*z*: 985.2 $[M+H]^+$. The spectroscopic data for **1C16** and **1C20** are presented in the Supporting Information.

Synthesis of hybrid mesostructures 1H: Hydrolysis of **1C*n*** was performed in a solution with a molar ratio of **1C*n***/THF/H_2O/HCl = 1:75:21:0.5. After stirring at room temperature for 7 days, the hydrolyzed solution was dropped onto glass substrates and slowly air-dried at room temperature. Silica-based hybrids (**1H**) were obtained as transparent thick films, which were scraped off from the substrates and pulverized. Also, **1H** was calcined at 500 °C for 8 h in air to remove organic moieties.

Characterization: The XRD patterns of the products were obtained on a Mac Science M03XHF22 diffractometer with Mn-filtered $Fe_{K\alpha}$ radiation. Transmission electron microscopy (TEM) observations were carried out on a JEOL JEM-2010 microscope operated at 200 kV. To prepare TEM samples, powders were ground with mortar and pestle and dispersed in ethanol. A carbon-coated copper grid was immersed in this dispersion and allowed to dry in air. Solid-state ^{29}Si MAS NMR spectra were recorded on a JEOL JNM-CMX-400 spectrometer at a resonance frequency of 79.42 MHz with a 45° pulse and a recycle delay of 100 s. For solid-state NMR measurements, the samples were put into 5 mm zirconia rotors and spun at 5 kHz. Liquid-state ^{29}Si NMR spectra of the precursor solutions containing $[D_8]$THF were recorded on a JEOL Lambda-500 spectrometer at a resonance frequency of 99.05 MHz with a pulse width of 6.5 μs, and 64 scans were acquired with a recycle delay of 30 s. Chemical shifts for ^{29}Si NMR were referenced to tetramethylsilane at 0 ppm. Nitrogen adsorption-desorption measurements were performed by an Autosorb-1 instrument (Quantachrome Instruments) at 77 K. The Brunauer–Emmett–Teller (BET) surface area was calculated from the adsorption branch in the relative pressure range from 0.02 to 0.05. The pore size distribution was evaluated using the non-local density functional theory (NLDFT) equilibrium model (N_2 at 77 K on silica, cylindrical pore).[26]

Acknowledgement

The authors are grateful to Prof. D. Mochizuki (Tokyo Institute of Technology) and Mr. Y. Hagiwara (Waseda University) for experimental help. This work was supported in part by a Grant-in-Aid for Scientific Research (No. 18350110) and the Global COE program "Practical Chemical Wisdom" from MEXT, Japan. K. K. also acknowledges the support by a Grant-in-Aid Scientific Research on Priority Areas "New Materials Science Using Regulated Nano Spaces, Strategy in Ubiquitous Elements" from MEXT, Japan. The A3 Foresight Program "Synthesis and Structural Resolution of Novel Mesoporous Materials" supported by the Japan Society for Promotion of Science (JSPS) is also acknowledged.

[1] For example; C. Sanchez, G. J. d. A. A. Soler-Illia, F. Ribot, T. Lalot, C. R. Mayer, V. Cabuil, *Chem. Mater.* **2001**, *13*, 3061–3083, and references therein.

[2] a) A. Shimojima, Y. Sugahara, K. Kuroda, *Bull. Chem. Soc. Jpn.* **1997**, *70*, 2847–2853; b) A. Shimojima, N. Umeda, K. Kuroda, *Chem. Mater.* **2001**, *13*, 3610–3616; c) A. Shimojima, K. Kuroda, *Chem. Rec.* **2006**, *6*, 53–63; d) A. Shimojima, C.-W. Wu, K. Kuroda, *J. Mater. Chem.* **2007**, *17*, 658–663.

[3] a) K. Katagiri, K. Ariga, J. Kikuchi, *Chem. Lett.* **1999**, 661–662; b) K. Katagiri, M. Hashizume, K. Ariga, T. Terashima, J. Kikuchi, *Chem. Eur. J.* **2007**, *13*, 5272–5281.

[4] L. D. Carlos, V. de Zea Bermudez, V. S. Amaral, S. C. Nunes, N. J. O. Silva, R. A. Sa Ferreira, J. Rocha, C. V. Santilli, D. Ostrovskii, *Adv. Mater.* **2007**, *19*, 341–348.

[5] a) B. Boury, R. J. P. Corriu, V. L. Strat, P. Delord, M. Nobili, *Angew. Chem.* **1999**, *111*, 3366–3370; *Angew. Chem. Int. Ed.* **1999**, *38*, 3172–3175; b) B. Boury, R. J. P. Corriu, *Chem. Commun.* **2002**, 795–802; c) B. Boury, R. Corriu, *Chem. Rec.* **2003**, *3*, 120–132.

[6] a) J. J. E. Moreau, B. P. Pichon, M. Wong Chi Man, C. Bied, H. Pritzkow, J.-L. Bantignies, P. Dieudonné and J.-L. Sauvajol, *Angew. Chem.* **2004**, *116*, 205–208; and J.-L. Sauvajol, *Angew. Chem.* **2004**, *116*, 205–208; *Angew. Chem. Int. Ed.* **2004**, *43*, 203–206; b) J. J. E. Moreau, L. Vellutini, M. Wong Chi Man, C. Bied, P. Dieudonné, J.-L. Bantignies, J.-L. Sauvajol, *Chem. Eur. J.* **2005**, *11*, 1527–1537; c) I. Karatchevtseva, D. J. Cassidy, M. Wong Chi Man, D. R. G. Mitchell, J. V. Hanna, C. Carcel, J. J. E. Moreau, J. R. Bartlett, *Adv. Funct. Mater.* **2007**, *17*, 3926–3932.

[7] a) Y. Luo, J. Lin, H. Duan, J. Zhang, C. Lin, *Chem. Mater.* **2005**, *17*, 2234–2236; b) L. Yang, P. Peng, K. Huang, J. T. Mague, H. Li, and Y. Lu, *Adv. Funct. Mater.* **2008**, *18*, 1526–1535.

[8] a) A. Shimojima, K. Kuroda, *Angew. Chem.* **2003**, *115*, 4191–4194; *Angew. Chem. Int. Ed.* **2003**, *42*, 4057–4060; b) A. Shimojima, Z. Liu, T. Ohsuna, O. Terasaki, K. Kuroda, *J. Am. Chem. Soc.* **2005**, *127*, 14108–14116.

[9] a) P. G. Harrison, *J. Organomet. Chem.* **1997**, *542*, 141–183; b) R. E. Morris, *J. Mater. Chem.* **2005**, *15*, 931–938, and references therein.

[10] a) C. A. Fyfe and G. Fu, *J. Am. Chem. Soc.* **1995**, *117*, 9709–9714; b) Firouzi, F. Atef, A. G. Oertli, G. D. Stucky, B. F. Chmelka, *J. Am. Chem. Soc.* **1997**, *119*, 3596–3610.

[11] L. Zhang, H. C. L. Abbenhuis, Q. Yang, Y.-M. Wang, P. C. M. M. Magusin, B. Mezari R. A. Santen, C. Li, *Angew. Chem.* **2007**, *119*, 5091–5094; *Angew. Chem. Int. Ed.* **2007**, *46*, 5003–5006.

[12] Y. Hagiwara, A. Shimojima, K. Kuroda, *Chem. Mater.* **2008**, *20*, 1147–1153.

[13] T. Cassagneau, F. Caruso, *J. Am. Chem. Soc.* **2002**, *124*, 8172–8180.

[14] a) G. H. Mehl, I. M. Saez, *Appl. Organomet. Chem. Appl. Organometal. Chem.* **1999**, *13*, 261–272; b) C. Zhang, T. J. Bunning, R. M. Laine, *Chem. Mater.* **2001**, *13*, 3653–3662; c) R. M. Laine, *J. Mater. Chem.* **2005**, *15*, 3725–3744.

[15] a) C.-M. Leu, T.-T. Chang, K.-H. Wei, *Macromolecules* **2003**, *36*, 9122–9127, b) C.-M. Leu, G. M. Reddy, K.-H. Wei, C.-F. Shu, *Chem. Mater.* **2003**, *15*, 2261–2265.

[16] a) R. Knischka, F. Dietsche, R. Hanselmann, H. Frey, R. Mülhaupt, *Langmuir* **1999**, *15*, 4752–4756; b) B.-S. Kim, P. T. Mather, *Macromolecules* **2002**, *35*, 8378–8384; c) K.-M. Kim, D.-K. Keum, Y. Chujo, *Macromolecules* **2003**, *36*, 867–875.

[17] C. Marcolli, G. Calzaferrit, *Appl. Organomet. Chem. Appl. Organometal. Chem.* **1999**, *13*, 213–226.

[18] a) G. Calzaferri, R. Imhof, K. W. Törnroos, *J. Chem. Soc. Dalton Trans.* **1994**, 3123–3128; b) J. Zhou, J. Kieffer, *J. Phys. Chem. C* **2008**, *112*, 3473–3481.

[19] X. Zhang, E. R. Chan, S. C. Glotzer, *J. Chem. Phys.* **2005**, *123*, 184718–184723.

[20] C. J. Brinker, G. W. Scherer, *Sol-Gel Science*, Academic Press, San Diego, **1990**.

[21] A. Saupe, *J. Colloid Interface Sci.* **1977**, *58*, 549–558.

[22] M. Klotz, P.-A. Albouy, A. Ayral, C. Ménager, D. Grosso, A. V. d. Lee, V. Cabuil, F. Babonneau, C. Guizard, *Chem. Mater.* **2000**, *12*, 1721–1728.

[23] a) J. N. Israelachvili, D. J. Mitchell, B. W. Ninham, *J. Chem. Soc. Faraday Trans. 2* **1976**, *72*, 1525–1568; b) Q. Huo, D. I. Margolese, G. D. Stucky, *Chem. Mater.* **1996**, *8*, 1147–1160.

[24] a) V. W. Day, W. G. Klemperer, V. V. Mainz, D. M. Millar, *J. Am. Chem. Soc.* **1985**, *107*, 8262–8264; b) W. G. Klemperer, V. V. Mainz, D. M. Millar, *Mater. Res. Soc. Symp. Proc.* **1986**, ***73***, 15–25; c) P. C.

 © 2008 Wiley-VCH Verlag GmbH & Co. KGaA, Weinheim

Cagle, W. G. Klemperer, C. A. Simmons, *Mater. Res. Soc. Symp. Proc.* **1990**, *180*, 29–37.
[25] L. A. Villaescusa, F. M. Márquez, C. M. Zicovich-Wilson, M. A. Camblor, *J. Phys. Chem. B* **2002**, *106*, 2796–2800.
[26] P. I. Ravikovitch, D. Wei, W. T. Chueh, G. L. Haller, A. V. Neimark, *J. Phys. Chem. B* **1997**, *101*, 3671–3679.
[27] P. A. Agaskar, *Inorg. Chem.* **1991**, *30*, 2707–2708.
[28] A. R. Bassindale, T. Gentle, *J. Organomet. Chem.* **1996**, *521*, 391–393.

Received: June 7, 2008
Published online: September 9, 2008

 © 2008 Wiley-VCH Verlag GmbH & Co. KGaA, Weinheim